Additively Fabricated Air-Filled Waveguide Integrated With Printed Circuit Board Using a Through-Patch Transition

Jakub Sorocki, *Member, IEEE*, Ilona Piekarz, *Member, IEEE*, Andrzej Samulak, Nicolo Delmonte, *Member, IEEE*, Lorenzo Silvestri, *Member, IEEE*, Stefania Marconi, Gianluca Alaimo, Ferdinando Auricchio, and Maurizio Bozzi, *Fellow, IEEE*

***Abstract*— The hybrid integration of an additively fabricated air-filled waveguide (WG) with a printed circuit board (PCB) is presented. An arrangement is proposed where different waveguiding structures share the same common metal plane on PCB. Such an approach allows combining the low-loss and high-Q properties of an air-filled waveguide, active circuit realization of the strip transmission line, and 3-D capabilities of additive manufacturing. A broadband transition is developed employing a through-patch coupling interface from a microstrip (MS) line to a waveguide. The concept was experimentally validated with exemplary transitions operating within X-band and K-band, featuring a measured bandwidth of $f_h/f_l \approx 1.4$ and average per-transition loss including connecting lines of ∼1.2 and ∼1.9 dB, respectively.**

***Index Terms*— Additive manufacturing (AM), K-band, printed circuits, transition, waveguide (WG) and printed circuit board (PCB) integration, X-band.**

I. Introduction

THE compact front-ends or their parts operating at high frequencies, especially at millimeter-waves (mm-waves) are mostly realized using substrate integrated waveguide (SIW), which can be fabricated using an industry-standard printed circuit board (PCB) process. However, despite many advantages, such circuits suffer from relatively high-power loss being a result of an electromagnetic (EM) wave propagating fully or partially within the lossy dielectric and/or low effective conductivity metallization [1], [2], especially at higher frequencies. An industry-standard technology that could be used to counteract those limitations is the utilization of air-filled waveguides (WGs), which feature very low power loss since transverse electric (TE) or transverse magnetic (TM) wave modes can propagate in lossless air filling. Recently, for such a waveguide realization, the additive manufacturing (AM) technology has already been proven to be well suited [3] in place of bulk metal milling and allows to reduce the cost of production and parts weight. However, usually, the waveguide components exist as stand-alone units and thus integration with PCB is an important research objective.

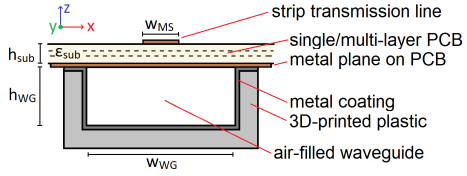

Fig. 1. Concept of an additively fabricated air-filled waveguide integrated with a PCB hosting a strip transmission line.

In this letter, we propose for the first time to the best of our knowledge, an additively fabricated air-filled waveguide integrated with the PCB. An arrangement is proposed where different waveguiding structures share the same common metal plane on PCB which serves on one side as a ground plane for the strip transmission line and on the other as one of the walls of the waveguide with others being a metalized U-shaped plastic. Such an approach allows combining the low-loss and high-Q properties of an air-filled waveguide, active circuit realization of the strip transmission line, and 3-D capabilities of AM. A broadband transition is developed employing a through-patch coupling and impedance matching step to interface the above guides. This concept has been experimentally validated with a fabricated microstrip (MS)-to-waveguide transition in back-to-back arrangement operating at X-band and K-band, respectively.

II. Wave Guiding Structures Realization in Hybrid PCB–AM Technology

A. Integration Concept

A conceptual drawing of the PCB integrated waveguide is presented in Fig. 1. The waveguide structure is realized as an attachment to the PCB taking advantage of one of the available copper metal layers. The proposed approach is a step beyond the industry standard stack-up where a microwave substrate hosting SIW structure is attached to a multilayer PCB (e.g., [4]), toward a more feature-packed next generation of mm-wave systems realization technology. The concept presented in Fig. 1 features many advantages

Manuscript received July 14, 2021; revised August 16, 2021; accepted September 11, 2021. Date of publication September 22, 2021; date of current version November 8, 2021. This work was supported in part by the National Science Center, Poland, under Grant 2019/34/E/ST7/00342. The work of Jakub Sorocki was supported by the Polish National Agency for Academic Exchange (NAWA) through the Bekker Program under Grant PPN/BEK/2019/1/00240. *(Corresponding author: Jakub Sorocki.)*

Jakub Sorocki and Ilona Piekarz are with the Institute of Electronics, AGH University of Science and Technology, 30-059 Kraków, Poland, and also with the Department of Electrical, Computer and Biomedical Engineering, The University of Pavia, 27100 Pavia, Italy (e-mail: jakub.sorocki@agh.edu.pl).

Andrzej Samulak resides in 90480 Nuremberg, Germany.

Nicolo Delmonte, Lorenzo Silvestri, and Maurizio Bozzi are with the Department of Electrical, Computer and Biomedical Engineering, The University of Pavia, 27100 Pavia, Italy.

Stefania Marconi, Gianluca Alaimo, and Ferdinando Auricchio are with the Department of Civil Engineering and Architecture, The University of Pavia, 27100 Pavia, Italy.

Color versions of one or more figures in this letter are available at https://doi.org/10.1109/LMWC.2021.3112567.

Digital Object Identifier 10.1109/LMWC.2021.3112567

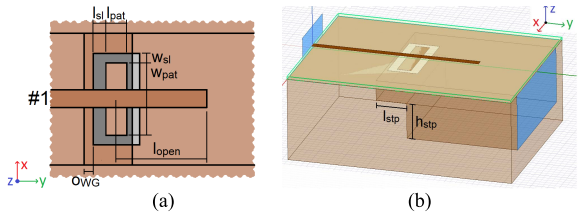

Fig. 2. (a) Top and (b) isometric view of the transition with main geometry parameters indicated. Wave propagation along Y-axis.

comparing to SIW. First, it allows minimizing dielectric-related power losses of the propagating wave compared to SIW by replacing a lossy substrate with a lossless air layer. Moreover, with the proposed construction, it is possible to minimize the use of thru-hole vias, as those increase fabrication costs and reduce accuracy compared to etching technology. The open U-shaped waveguide was designed to simplify the AM fabrication process (including metallization) and enable low-cost fabrication of waveguide circuits with fine details using industry-standard technologies such as Direct Light Processing or PolyJet Printing (tens of micrometer resolution). It must be noted, in the presented approach, simple integration of waveguide and strip transmission line circuits is possible as well as there is a possibility to minimize the unwanted coupling of active circuitry to, e.g., filters or feeding networks as well as shielding them from the radiation of, e.g., antenna arrays as the two can be located on different sides of the PCB metal plane.

B. Microstrip Line to Air-Filled Waveguide Transition

The introduction of the hybrid stack-up is accompanied by the presentation of a strip transmission line to air-filled waveguide transition. A variety of transition designs presented in the literature, i.e., vertical probe-feeding [5], patch-coupling type [6], or inline waveguide ridge [7] were studied and none suited the application fully. Thus, a new broadband transition layout is proposed, which takes advantage of through-ground-patch coupling and provides parallel orientation on the opposite sides of a ground plane of the two guides. A drawing of the proposed transition is shown in Fig. 2(a) and (b). The waveguide was integrated with the PCB through its broad wall and the wave propagates along the Y-axis. An open stub in MS is used along with a height step in the waveguide for matching and broadband operation. A shorted stub could also be used at the expense of extra vias and more difficult performance tuning.

The design procedure for the transition should be as follows. First, the patch width w_{pat} and the MS line open stub length l_{open} (see Fig. 2) should be assumed to be equal $\lambda_g/2$. The initial value for patch length l_{pat} can be chosen to be $\lambda_g/8$. The separations between the patch and the ground plane l_{sl}, w_{sl} can be freely chosen depending on the fabrication limits and the waveguide size. In the next step, w_{pat} needs to be adjusted to obtain the transition operating at the desired center frequency. Moreover, l_{open}, l_{sl}, and w_{sl} need to be tuned to achieve possibly the best impedance match seen from the MS transmission line port. The improvement of the impedance match seen from the waveguide side can be achieved by adding an extra step [see Fig. 2(b)] decreasing the impedance mismatch between the MS line and an air-filled waveguide. The initial height h_{stp} and width w_{stp} of the step can be assumed to be equal $\lambda_g/4$ and $2l_{\text{sl}} + l_{\text{pat}}$. Finally, h_{stp} and l_{pat} can be tuned to improve the impedance match seen from the waveguide side.

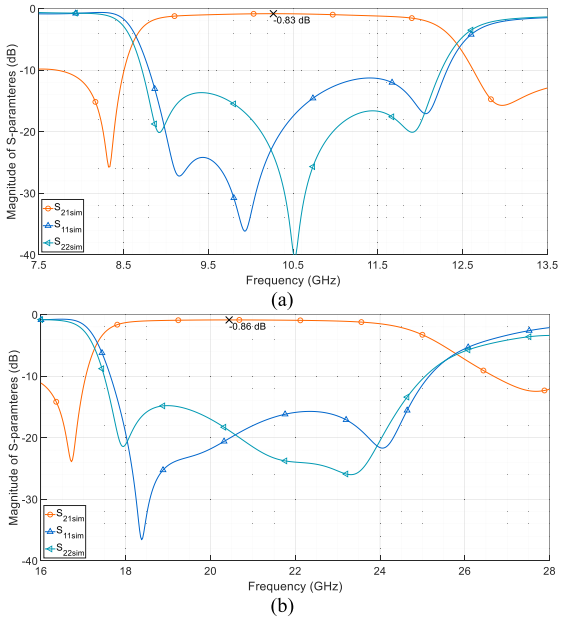

Fig. 3. EM simulated S-parameters of the transitions operating in (a) X-band and (b) K-band. Port #1 is the MS side, #2 is the waveguide side.

TABLE I
DIMENSIONS (mm) FOR MICROSTRIP-TO-WAVEGUIDE TRANSITIONS

	Name	X-b.	K-b.		Name	X-b.	K-b.
w_{MS}	MS width	1.16	0.69	h_{WG}	WG height	10.16	4.32
w_{sl}	Slot width	1	0.8	w_{WG}	WG width	22.86	10.67
w_{pat}	Patch width	11	4.9	o_{WG}	WG end offset	0.5	0.1
l_{sl}	Slot length	1.5	0.9	l_{open}	MS end length	14.7	6.1
l_{pat}	Patch length	2.5	1.2	h_{stp}	WG step height	6.5	2.9/0.8
				l_{stp}	WG step length	5.5	2.5/2.5

Broadband operation is achieved by exciting three separate resonances (two from the patch and one from the open stub) across the passband that ensure energy transfer. Also, matching can be further improved by adding a second step in the waveguide as done for the K-band transition.

III. EXPERIMENTAL RESULTS

Two exemplary transitions were designed to verify the proposed concept, i.e., one operating at X-band with the center frequency of $f_0 = 10.5$ GHz and the second one operating at K-band with the center frequency of $f_0 = 22$ GHz. Standard waveguide sizes of WR-90 and WR-42 were assumed to operate at fundamental TE_{10} propagation mode. Double-sided circuit boards were fabricated on a 20 and 12 mil thick Rogers RO4003C microwave laminate ($\varepsilon_r = 3.38$, $\tan\delta = 0.0027$ at 10 GHz) for X-band and K-band, respectively. A MS feeding was used to simplify the fabrication at the expense of increased insertion losses as when no top ground plane is present, the slot might partially radiate in the unwanted direction away from the waveguide. The final dimensions listed in Table I were found in *Ansys HFSS* software through the optimization process of the full-wave EM model. The resulting S-parameters are shown in Fig. 3. Different behavior between the MS and the waveguide ports is observed which is unavoidable for this type of transition. The total power loss ($\text{TPL} = 1 - |S_{21}|^2 - |S_{11}|^2$) at f_0 of X-/K-band is 0.75 dB/0.79 dB with major contribution of radiation loss 0.63 dB/0.65 dB.

The following process was used for manufacturing the transitions in a back-to-back configuration. The PCBs were manufactured using the photolithography method and chemical

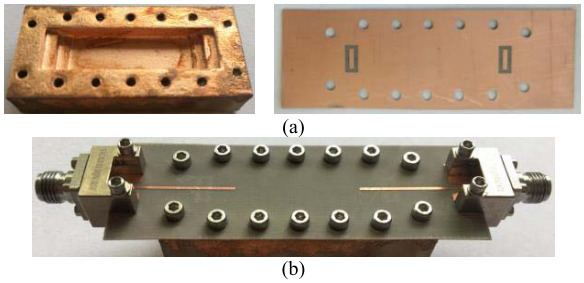

Fig. 4. Photographs of the fabricated K-band circuit: (a) copper-printed waveguide and PCB's metal plane with coupling slots and (b) full assembly.

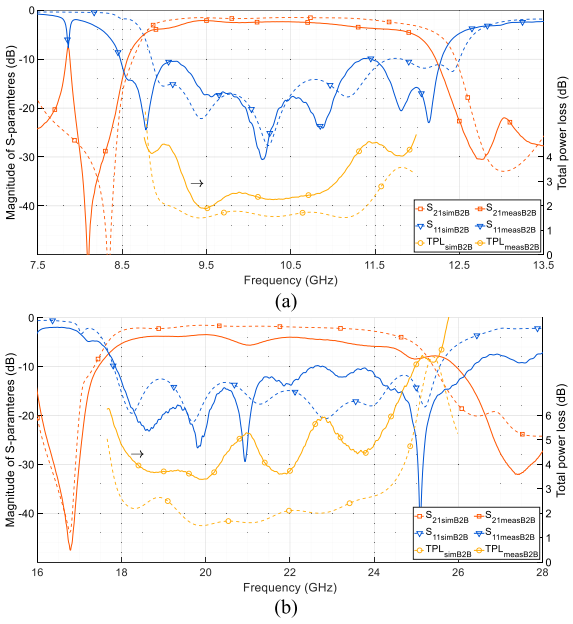

Fig. 5. Measured S-parameters of (a) X-band and (b) K-band demonstrators in back-to-back (solid lines) versus EM data (dashed lines). TPL overlayed.

etching. A set of corresponding holes was placed on the PCB and the 3-D printed part to accept the alignment pins and to screw together the two parts providing pressure-assisted low resistance contact between metals. This was followed by AM fabrication of the waveguide parts in a two-step process. At first, the plastic shells were 3-D printed out of UV-cured resin using the Original Prusa SL1 M-stereolithography (SLA)-type printer (pixel size of 47 μm) at 100μm layer height. Models' parts were placed directly on the build platform to ensure maximally flat and even X–Y surfaces which are crucial for achieving good effective conductivity of the ground plane. Then, the plastic shells were coated with metal. The electroplating process was used after coating the parts with conductive paint, to grow roughly a 5μm thick copper layer. Finally, the circuits were assembled, and 3.5 mm coax end-launch connectors were attached. Photographs of the fabricated demonstrator are shown in Fig. 4.

The circuits were measured using the Agilent PNA Network Analyzer N5227 at 10 MHz steps with the reference plane set at the connectors' plane. The collected S-parameters are provided in Fig. 5 with the EM calculated data overlayed (being equivalent to classic waveguide fabrication; smooth copper, lossless contact assumed). It is seen that the fabricated X-band transition operates within 8.85–12.35 and 17.8–26.0 GHz bandwidth with an impedance match better than −8 dB and an average per-transition insertion loss of ∼1.2 and ∼1.9 dB (note this includes 15 mm of the MS line and 35 mm/20 mm

TABLE II

SUMMARY OF THE PROPERTIES AND PERFORMANCE OF VARIOUS MICROSTRIP-TO-WAVEGUIDE TRANSITIONS

	Transition	Feed vs. WG	Vias	Loss per transition#	BW* f_h/f_l	WG fabric.	Freq. band
[6]	MS-WG	Perpend.	yes	< 0.4 dB	1.2	MM	E
[8]	MS-WG	Inline	no	< 0.9 dB	1.5	MM	X
[9]	MS-WG	Perpend.	yes	< 1.4 dB	1.2	MM	Ka
[10]	MS-WG	Inline	no	< 1 dB	1.05	MM	E
[11]	MS-SIW	Parallel	yes	< 1.3 dB	1.6	SIW	Ka
[12]	MS-WG	Parallel	no		2	MM	C
This	MS-WG	Parallel	no	1.1 – 2.0 dB	1.4	C3Dp	X
This	MS-WG	Parallel	no	1.7 – 3.9 dB	1.46	C3Dp	K

MM – metal milling, C3Dp – coated 3D print

of the WG). The hybrid waveguide only losses are estimated to be below 0.1 dB/cm (waveguide propagation constant was deembedded using an extra circuit with the same transitions and different waveguide lengths); however, an exact number is hard to establish due to fabrication tolerances and low losses. The performance drop and increased TPL compared to EM data may be attributed to finite fabrication tolerances, reduced metal conductivity due to surface roughness, and nonzero PCB-WG contact resistance, all resulting from the used fabrication technology and assembly procedure. The latter is especially important since the contact with the PCB is in the waveguide's region of higher current concentration, mainly in the MS to WG launch region and secondarily in the WG narrow and broad wall seam. Mating two rough metal surfaces may result in a nonuniform galvanic contact leading to distorted current distribution and thus increased power losses. Proper clamping and/or smoothing the interface reduce the above. Importantly, the K-band transition poses more strict requirements (generally increasing the operating frequency) for fabrication as compared to X-band due to its smaller size along with the need for a smoother metal surface to minimize conductor losses as the skin depth is shallower. No direct power coupling due to open stubs facing each other was expected. The proposed transitions were compared with other solutions in the literature with a summary provided in Table II. As seen, the transitions feature easy integration with PCBs, low-cost realization due to the use of AM process, and no requirements for vias as well as relatively wide operational bandwidth and low insertion losses.

IV. CONCLUSION

A novel concept of hybrid integration of additively manufactured air-filled waveguide with PCB technology was proposed. The structure combines the low losses of the air-filled waveguide structure, active circuitry integration of PCB technology, and 3-D flexibility of AM. A broadband transition from MS to waveguide was introduced as well. Exemplary circuits operating at X-band and K-band were fabricated and measured to experimentally validate the performance of the proposed approach. The obtained results have shown the potential toward the realization of a more feature-packed next generation of mm-wave circuits and systems.

REFERENCES

[1] F. Parment, A. Ghiotto, T. P. Vuong, J. M. Duchamp, and K. Wu, "Broadband transition from dielectric-filled to air-filled substrate integrated waveguide for low loss and high-power handling millimeter-wave substrate integrated circuits," in *IEEE MTT-S Int. Microw. Symp. Dig.*, Tampa, FL, USA, Jun. 2014, pp. 1–3.

[2] F. Parment, A. Ghiotto, T. P. Vuong, J. M. Duchamp, and K. Wu, "Air-filled substrate integrated waveguide for low-loss and high power-handling millimeter-wave substrate integrated circuits," *IEEE Trans. Microw. Theory Techn.*, vol. 63, no. 4, pp. 1228–1238, Apr. 2015.

[3] J. Shen and D. S. Ricketts, "Additive manufacturing of complex millimeter-wave waveguides structures using digital light processing," *IEEE Trans. Microw. Theory Techn.*, vol. 67, no. 3, pp. 883–895, Mar. 2019.

[4] APTIV Services US LLC. (Sep. 2020). *76 to 77 GHz Vehicular Radar SRR3, United States Federal Communications Commission Certification Documentation*. Accessed: Nov. 26, 2020. [Online]. Available: https://fccid.io/L2C0059TR

[5] T. Q. Ho and Y.-C. Shih, "Spectral-domain analysis of E-plane waveguide to microstrip transitions," *IEEE Trans. Microw. Theory Techn.*, vol. 37, no. 2, pp. 388–392, Feb. 1989.

[6] N. T. Tuan, K. Sakakibara, and N. Kikuma, "Bandwidth extension of planar microstrip-to-waveguide transition by controlling transmission modes through via-hole positioning in millimeter-wave band," *IEEE Access*, vol. 7, pp. 161385–161393, Nov. 2019.

[7] H. W. Yao, A. Abdelmonem, J. F. Liang, and K. A. Zaki, "Analysis and design of microstrip to waveguide transitions," *IEEE Trans. Microw. Theory Techn.*, vol. 42, no. 12, pp. 2371–2379, Dec. 1994.

[8] N. Kaneda, Y. Qian, and T. Itoh, "A broad-band microstrip-to-waveguide transition using quasi-Yagi antenna," *IEEE Trans. Microw. Theory Techn.*, vol. 47, no. 12, pp. 2562–2567, Dec. 1999.

[9] A. Mozharovskiy, S. Churkin, A. Arternenko, and R. Maslcnnikov, "Wideband probe-type waveguide-to-microstrip transition for 28 GHz applications," in *Proc. 48th Eur. Microw. Conf. (EuMC)*, Madrid, Spain, Sep. 2018, pp. 113–116.

[10] B. Boukari, E. Moldovan, S. Affes, K. Wu, R. G. Bosisio, and S. O. Tatu, "Robust microstrip-to-waveguide transitions for millimeter-wave radar sensor applications," *IEEE Antennas Wireless Propag. Lett.*, vol. 8, pp. 759–762, 2009.

[11] T. Y. Huang, T. M. Shen, and R. B. Wu, "Design and modeling of microstrip line to substrate integrated waveguide transitions," in *Passive Microwave Components and Antennas*, vol. 11. London, U.K.: IntechOpen, 2010, pp. 225–246.

[12] X. Huang and K.-L. Wu, "A broadband U-slot coupled microstrip-to-waveguide transition," *IEEE Trans. Microw. Theory Techn.*, vol. 60, no. 5, pp. 1210–1217, May 2012.